Baseline and Projected Future Carbon Storage and Carbon Fluxes in Ecosystems of Hawai‘i
Editors: Paul C. Selmants, Christian P. Giardina, James D. Jacobi, and Zhiliang Zhu
U.S. Geological Survey Professional Paper 1834, 2017

Chapter 3. Projecting End-of-Century Shifts in the Spatial Pattern of Plant-Available Water Across Hawai‘i to Assess Implications to Vegetation Shifts

By Lucas B. Fortini,[1] James D. Jacobi,[1] and Jonathan P. Price[2]

3.1. Highlights

- Anticipating potential shifts in plant communities has been a major challenge in climate change ecology. In Hawai‘i, where conservation efforts tend to be habitat focused, the lack of projections of vegetation shifts under future climate is a major knowledge gap for developing management actions aimed at climate change mitigation and adaptation.
- As a first approximation of such changes, we have modeled potential shifts of terrestrial vegetation across the Hawaiian landscape between now and the end of this century. Our approach relies on modeling the relation between current climate and the distribution of broad, climatically determined moisture zones (for example, dry, mesic, and wet areas) that form the basis of natural land-cover classification classes in Hawai‘i (for example, dry forests, wet forests, mesic shrublands).
- In this approach we modeled the suitability of the landscape to each moisture zone based on its relation to mean annual temperature, wet season precipitation, and dry season precipitation and then integrated these individual moisture-zone models into landscape moisture-zone projections under current and end-of-century climate scenarios.
- We integrated our moisture-zone projections into a detailed Hawai‘i land-cover map to derive a first approximation of climate-based shifts in land cover in Hawai‘i. The results show we can accurately replicate the current distribution of Hawaiian moisture zones using simple climate metrics based on temperature and precipitation.
- Our resulting models identify areas in the landscape where projected shifts in climate may lead to moisture-driven vegetation shifts with clear consequences to overall carbon storage across the archipelago.

[1]U.S. Geological Survey.

[2]University of Hawai‘i at Hilo.

3.2. Introduction

Sharp climate and elevation gradients in the main Hawaiian Islands lead to huge vegetation variation over relatively short distances. Hawai‘i possesses 25 of the 35 Holdridge global life zones (Asner and others 2005), which results in large variability in biomass across the Hawaiian landscape (Asner and others, 2009, 2011). This variability means potential climate shifts can have major implications to land carbon through shifts in Hawai‘i vegetation distribution. An important step in quantifying the potential changes in carbon storage owing to projected climate shifts is quantifying how the vegetation may change over time under future scenarios. However, projecting potential shifts in vegetation and plant communities has been a major challenge in climate change research (Cramer and others, 2001). There are clear implications of such shifts to the conservation of Hawaiian native species and their habitat, especially given the number of endangered species in Hawai‘i and their high vulnerability to climate change (Fortini and others, 2013, 2015; Krushelnycky and others, 2013). This gap in knowledge of potential vegetation shifts in response to climate also hinders the quantification of shifts in potential landscape carbon storage that can allow for evaluation of the viability of carbon sequestration efforts (Bachelet and others, 2001; Lucht and others, 2006; Gibbs, 2007).

For a relatively small isolated land area such as Hawai‘i, there are few research approaches available to help us explore the potential climate-based shifts in vegetation. Vegetation-distribution projections based on global vegetation models do not typically apply to isolated islands. Although part of the reason is the coarse spatial resolution of most global vegetation models (Bonan and others, 2003; Gonzalez and others, 2010; Pavlick and others, 2013), another major challenge arises from the numerous differences among island and continental systems under which vegetation models are parameterized. For instance, isolated disharmonic flora (Ziegler, 2002), which lead to differences in species richness (Ostertag and others, 2014), fire prevalence and behavior (Benoit and others, 2009; Ellsworth and others, 2013), and ongoing biological invasions (Asner and others, 2008; Mascaro and others, 2008), indicate mechanistic models parameterized for continental systems are of limited applicability to Hawai‘i and other isolated archipelagos.

Given the lack of data necessary for the proper parameterization of mechanistic vegetation models in Hawai‘i and other similarly isolated islands (Hartig and others, 2012), we attempt to provide a coarse first approximation of the impacts of projected climate shifts to vegetation across Hawai‘i using a simple yet novel approach. Our approach relies on modeling the relation between current climate and the distribution of broad climatically determined moisture zones that form the basis of natural land-cover classification classes in Hawai‘i (for example, dry forests, wet forests, mesic shrublands; Gagne and Cuddihy, 1990; Gon, 2006; Rollins, 2009; Price and others, 2012). In this approach we first model the suitability of the landscape to each moisture zone based on variability of mean annual temperature (MAT), wet season precipitation, and dry season precipitation and then integrate these individual models into landscape moisture-zone projections under current and end-of-century climate scenarios. Additionally, we use a novel calibration algorithm to ensure unbiased projections of prevalence among modeled moisture-zone classes under current and future climate. Lastly, to approximate how these shifts in moisture zone may differentially impact forests, shrublands, and grasslands across Hawai‘i and their carbon storage potential, we integrate our moisture-zone projections to a Hawai‘i GAP Analysis Program (HIGAP) vegetation structure map (Jacobi and others, this volume, chap. 2).

3.3. Input Data and Methods

3.3.1. Land-cover Data and Processing

As baseline data for our projections, we used the map of current distribution of moisture zones across Hawai‘i (Price and others, 2012). The moisture-zone map describes the variability of plant-available moisture across Hawai‘i and has been used in most recent land-cover mapping efforts for the islands. This moisture-zone classification is primarily based on annual precipitation and potential evapotranspiration (thus also being a function of temperature and humidity), but also considers the distribution of independently derived vegetation moisture zones (Jacobi, 1989). The moisture-zone map is based on three generalized moisture classes (dry, mesic, and wet) that reflect the way vegetation types are commonly subcategorized in Hawai‘i (for example, wet versus mesic forests). In broad terms these moisture classes can be described as areas where the difference between mean annual precipitation (MAP) and potential evapotranspiration (PET) is more than 1,661 mm (wet), between 0 and 1,660 mm (mesic), and less than 0 mm (dry) (Price and others, 2007). Prior to all analyses, we resampled the moisture-zone map to 500-m pixel resolution using a majority filter to reduce the computational time required to run models (fig. 3.1).

3.3.2. Projecting Moisture-Zone Distributions Under Current and Future Climate

We projected current and future distribution of moisture zones across the Hawaiian Islands using an approach based on the comparative suitability of the Hawaiian landscape to each of the three moisture zones considered. In this approach, we create baseline and end-of-century landscape projections based on multiple iterations of our moisture-zone model (fig. 3.2). Each iteration of the model uses a stratified random sample of the baseline map (the training set) to determine the suitability of the landscape to each moisture zone based on climate predictors alone (individual moisture-zone models) using a boosted regression tree approach (BRT; fig. 3.3). Hence, individual iterations only provide partial coverage of landscape under current climate because projections are not applied to parts of landscape used for model fitting to avoid overfitting. We chose BRT based on the method’s overall good performance in similar efforts to model ecological distribution patterns (Elith and others, 2008; Hastie and others, 2011). An initial test showed similar accuracies for moisture-zone models based on simpler Mahalanobis distance-based methods. However, owing to the smaller computational requirements and wider acceptability of BRT, we used BRT for the remainder of our reported models. BRT is an increasingly common ecological modeling method frequently used in species distribution modeling owing to its good model fits. To merge individual moisture-zone models into a single projection (a multi-moisture-zone projection), we used a simple algorithm that assigns a moisture zone to each landscape cell based simply on which moisture zone has the highest model-derived suitability for that location (fig. 3.4). Comparisons with a simpler multinomial BRT approach showed that it provided less accurate and more biased model outputs compared to our approach.

All individual BRT models use optimal settings found in preliminary tests including using a 0.01 learning rate, a tree complexity of 5, and a 0.5 bag fraction (Elith and others, 2008). The number of trees in each model was optimized to balance predictive power versus generalization of models (Hijmans and others, 2012). All models and analyses were developed in the R programming language (R Core Team, 2014) using the dismo, gbm, and raster packages (Ridgeway, 2005; Hijmans and others, 2012, 2014)

3.3.2.1. Model Replicates

To limit the effect of individual training points to projection outcomes, we ran each model step 200 times using 80 percent of the baseline moisture-zone map for model fitting (the training set, n=51,992) and 20 percent for model evaluation (the evaluation set, n=12,998). Each model iteration splits the data using a stratified random sampling algorithm with respect to moisture-zone prevalence across islands in the original baseline map. Our approach was based on two sets of model runs (see Moisture-zone model workflow box below): a first step used to fit and calibrate our models (see section 3.3.2.2; figs. 3.2 through 3.4) and a second step to apply

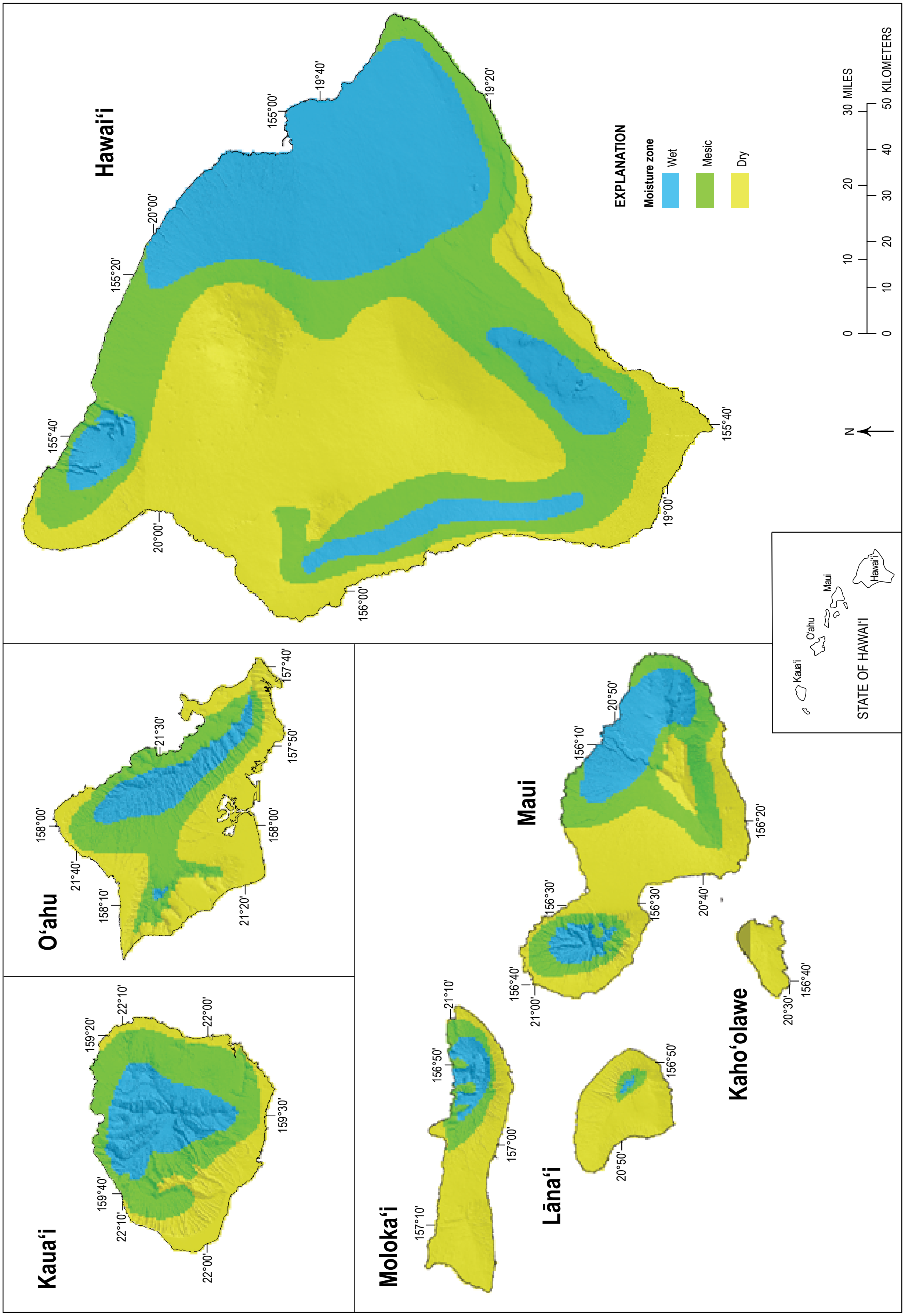

Shaded-relief base modified from U.S. Geological Survey National Elevation Dataset, 2015.

Figure 3.1. Baseline maps of moisture-zone distribution based on three classes commonly used to categorize Hawaiian vegetation.

Figure 3.2. Diagram illustrating the combination of multiple partial-coverage landscape moisture-zone projections into a final landscape moisture-zone projection. Final projection values are based on most frequent moisture-zone projection across iterations for each raster cell. MZ, moisture zone.

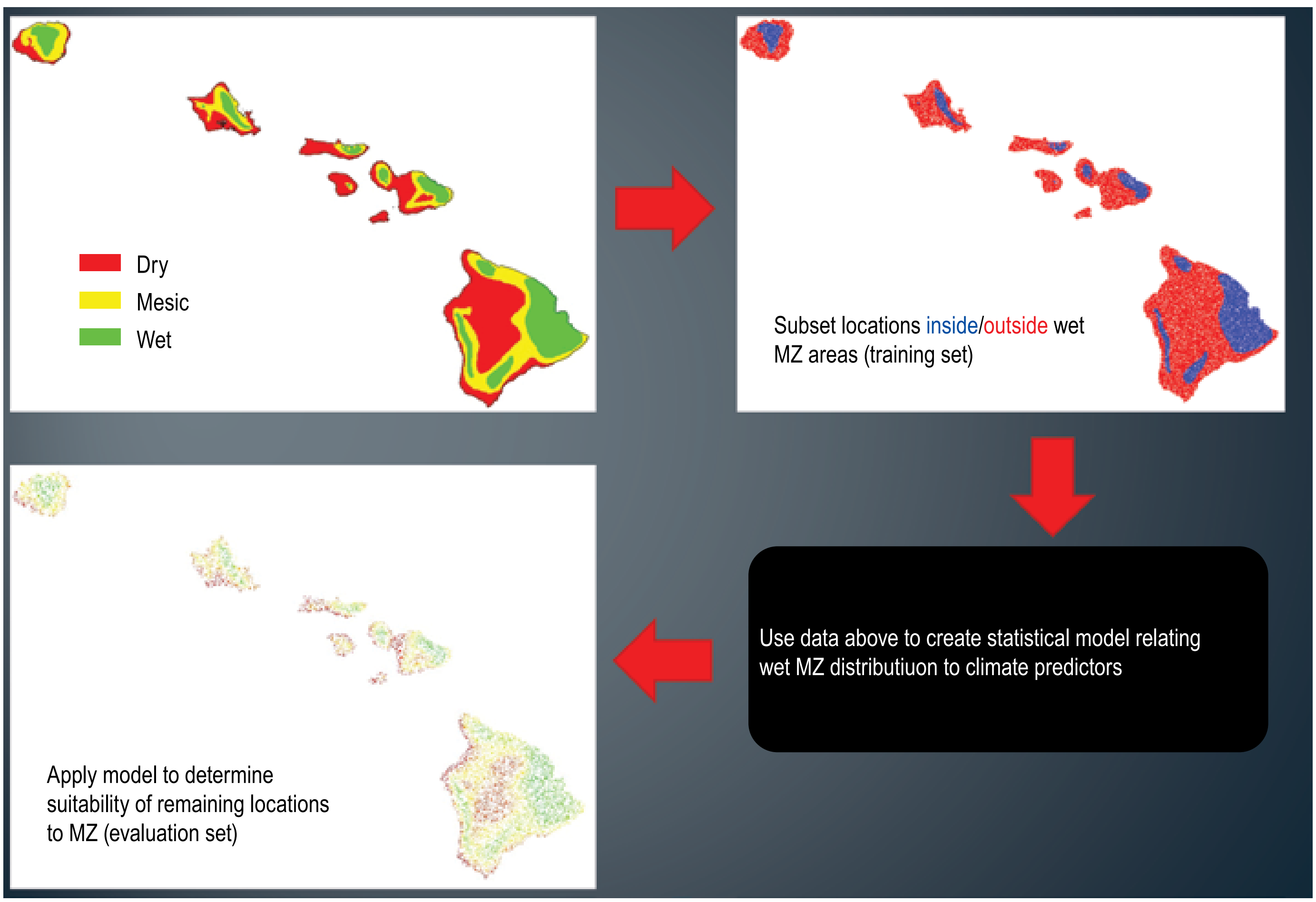

Figure 3.3. Diagram illustrating the fitting of the model describing the suitability of the landscape to individual moisture zones. This process uses the baseline moisture-zone map (fig. 3.1) for model training and evaluation. MZ, moisture zone.

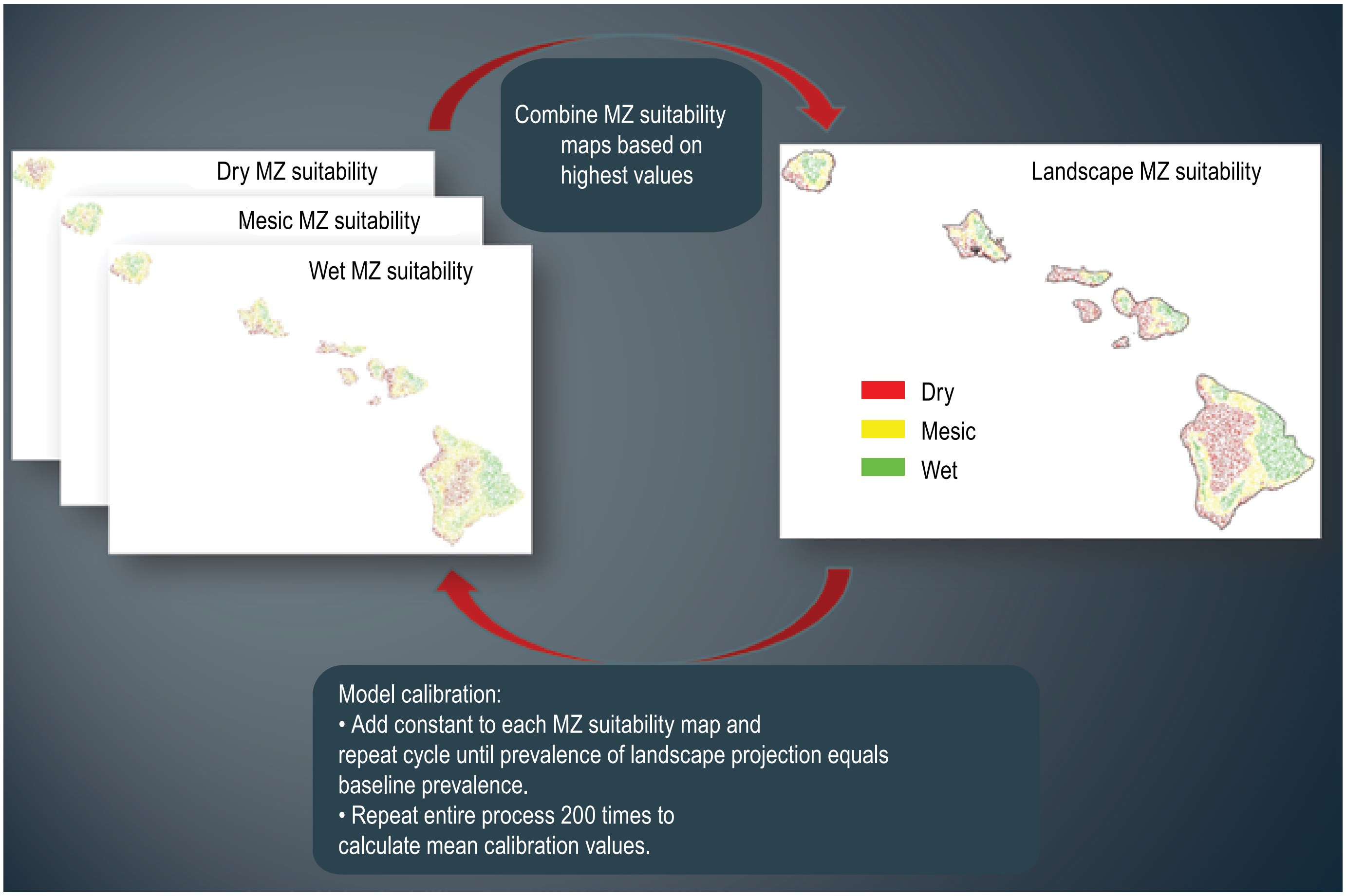

Figure 3.4. Diagram illustrating the integration of individual moisture-zone suitability models (fig. 3.2) into landscape moisture-zone projections. This iterative procedure includes a calibration step to minimize bias in landscape projections. Resulting Landscape moisture-zone projections do not have 100 percent landscape coverage as locations used for model fitting are excluded from output maps. MZ, moisture zone.

Moisture-zone model workflow:

Step 1: Model fitting and calibration under current climate (200 iterations)

- For each iteration:
    - Randomly split baseline cover and predictor maps into training (80 percent) and evaluation (20 percent) sets
    - For each moisture zone (fig. 3.2):
        - Fit BRT model using training set
        - Create moisture-zone suitability map using fitted model and evaluation set
    - Create landscape moisture-zone projection based on all moisture-zone suitability maps (fig. 3.3)
    - Calibrate landscape projection so its biome prevalence equals baseline prevalence
- Create mean calibration constants from all fitting and calibration iterations

Step 2: Model projections for baseline and future scenarios (200 calibrated runs, fig. 3.4)

- For each model iteration (baseline and future scenarios):
    - Re-apply moisture zone fitted models with mean calibrations
        - To current climate dataset
        - To future climate dataset

Step 3: Create final current and future landscape projections

- Create final maps based on most frequent moisture-zone projection across model runs the calibrated models under current and future climate to create our final landscape moisture-zone projections (see section 3.3.2.3; fig. 3.2).

3.3.2.2. Model Calibration Runs

Although the winner-takes-all approach to integrate multiple vegetation models into a single landscape model has been previously used (Tovar and others, 2013), we introduce a novel and simple calibration procedure that aims to minimize bias in final projections (fig. 3.3). This is necessary because there may be differences in model sensitivity and fit across individual moisture zones that could lead to bias in a final landscape classification. If this bias is consistent across model iterations, a standard model averaging approach will not reduce it. Hence, in this procedure, after evaluating current moisture-zone projection bias in terms of deviations in moisture-zone prevalence between baseline moisture-zone distribution and current model projections for the evaluation set, a search algorithm incrementally adds or subtracts a constant to the suitability scores of each individual moisture zone until the subsequent landscape moisture-zone projection has prevalence across moisture zones within 1 percent of baseline prevalence. This calibration routine is analogous to presence/absence thresholding algorithms commonly used in species distribution models aimed at yielding projections with equal omission and commission errors (Jiménez-Valverde and Lobo, 2007; Liu and others, 2011). We repeated the model fitting, evaluation, and calibration steps 200 times using different evaluation and training sets to determine the final average model calibration constants to be applied in all calibrated final models.

3.3.2.3. Calibrated Model Runs and Final Projections

Following calibration, we projected 200 replicates of our model across the archipelago based on our current and future climate predictors, along with the average calibration values calculated above (fig. 3.4). The output of individual replicates does not yield a complete moisture-zone coverage map for current climate as the calibrated model is not applied to the training set locations to avoid overly confident projections. However, as each model replicate assigns the most likely moisture zone for 20 percent of the landscape, the final mean landscape projection under current and future climate is based on the most frequently predicted moisture zone for a given location. Lastly, we quantify uncertainty in our final model projections by calculating the ensemble committee agreement across all model iterations. This is calculated as the frequency at which the projected cover for a location is projected across all model replicates, where, for instance, a value of 0.8 indicates that 80 percent of model iterations assigned the same moisture zone to a given location.

3.3.2.4. Projection Integration with Land Cover

To determine the implications of moisture-zone changes to Hawaiian land cover, we integrated our current and future moisture-zone projections with a coarse vegetation map based on the carbon assessment for Hawai‘i (CAH) land-cover map by Jacobi and others (this volume, chap. 2). The CAH map is a detailed representation of current vegetation distribution across the main Hawaiian Islands based on multiple data sources resulting in 48 cover classes. As with other Hawaiian land-cover maps (Rollins, 2009), the CAH land-cover map stratifies most non-anthropogenic cover types into moisture-zone subclasses. For the purpose of our simplistic land-cover analysis, we grouped the original classes into forest, shrubland, and grassland general classes resampled to 500-m resolution, excluding all original CAH land-cover classes that did not clearly fit into these three categories (table 3.1). This step not only simplified cover types considered but also removed all moisture-zone associations from the HIGAP map. We then simply merged our modeled moisture-zone map with the moisture-less HIGAP map using either the current or future moisture-zone projections. This overlay analysis allowed us to get a first approximation of the differential impact of projected moisture-zone shifts in forest, shrubland, and grassland areas across the state.

3.3.3. Environmental Predictors

We derived all climatic variables used as predictors in our models from current and future monthly temperature minimums and maximums (Tmin, Tmax) and precipitation data. We obtained current monthly precipitation and Tmin and Tmax data from 250-m resolution datasets (Giambelluca and others, 2013, 2014). We calculated mean annual wet season (November–April) and dry season (May–October) temperature and precipitation using the R package “raster” based on the monthly rainfall and temperature data (Hijmans and others, 2014). We calculated future yearly and seasonal climatic indicators using the same procedure as for the baseline data. However, before calculating yearly and seasonal indicators we derived the end-of-century values for monthly Tmin, Tmax, and precipitation by integrating climate projections with current climate estimates. To do that, we first calculated the projected change between 1990 and 2010 and between 2080 and 2100 for each monthly variable developed from the Hawaiian Regional Climate Model (HRCM) with 1-km spatial resolution for Maui and 3 km for all other islands (Zhang and others, 2012). We then added these delta values to current monthly climate values before recalculating all yearly and seasonal variables. The HRCM-based climate projections show an average of 2.5 °C warming over the islands, but with a clear increased warming at higher versus lower elevations (3.4 °C versus 2.2 °C, respectively), as documented in previous studies (Beniston and others, 1997; Diaz and Bradley, 1997; Rangwala and others, 2013). Predicted precipitation shifts include increased precipitation in windward wet areas of Hawai‘i and Maui, but general slight drying trends across the drier areas of the State.

The HRCM is based on the Weather Research and Forecasting model ver. 3.3 and uses the SRES A1B emission scenario and the mean of multiple CMIP3 global circulation

Table 3.1. Revised Hawai‘i GAP Analysis Program cover classes and their relation to our simplified land-use map integrated with current and future moisture-zone maps.

[Data from Jacobi and others (this volume, chap. 2). HIGAP, Hawai‘i GAP Analysis Program]

HIGAP cover class	Simplified cover class	HIGAP cover class	Simplified cover class
Alien dry forest	Forest	Alien mesic grassland	Grassland
Alien mesic forest	Forest	Alien wet grassland	Grassland
Alien wet forest	Forest	Native Deschampsia grassland	Grassland
Closed Hala forest	Forest	Native bog community	Other
Closed koa–ohia mesic forest	Forest	Wetland vegetation	Other
Closed koa–ohia wet forest	Forest	Cultivated agriculture	Other
Closed ohia dry forest	Forest	Developed open space	Other
Closed ohia mesic forest	Forest	Low–intensity developed	Other
Closed ohia wet forest	Forest	Medium–intensity developed	Other
Kiawe dry forest and shrubland	Forest	High–intensity developed	Other
Low-stature ohia wet forest	Forest	Very sparse vegetation to unvegetated	Other
Mixed native–alien dry forest	Forest	Water	Other
Mixed native–alien mesic forest	Forest	Alien dry shrubland	Shrubland
Mixed native–alien wet forest	Forest	Alien mesic shrubland	Shrubland
Native mesic to dry forest and shrubland	Forest	Alien wet shrubland	Shrubland
Open koa–mamane dry forest	Forest	Mixed native–alien dry cliff community	Shrubland
Open koa–ohia mesic forest	Forest	Mixed native–alien mesic shrubs and grass	Shrubland
Open koa–ohia wet forest	Forest	Mixed native–alien wet shrubs and grasses	Shrubland
Open ohia dry forest	Forest	Native wet cliff community	Shrubland
Open ohia mesic forest	Forest	Native dry shrubland	Shrubland
Open ohia wet forest	Forest	Native mesic shrubland	Shrubland
Mixed mamane–naio-native trees dry woodland	Forest	Native wet shrubland	Shrubland
Plantation forest	Forest	Uluhe ferns and native shrubs	Shrubland
Alien dry grassland	Grassland	Coastal strand vegetation	Shrubland

models (GCMs) (Zhang and others, 2012). The HRCM projections are based on a substantial regional dynamic climate model which replicates the regional and island climate mechanisms that largely dictate local climate, such as extreme orographic-based precipitation gradients and trade-wind inversions (Zhang and others, 2012). Because of computational limitations, only a single end-of-century climate projection is available from the HRCM. Although this limits our analysis to consider a single future climate scenario, without this downscaled effort, preliminary analysis showed available GCM outputs commonly used elsewhere are too coarse to represent the steep environmental gradients present across the archipelago.

We selected MAT, wet season precipitation, and dry season precipitation as our three predictors of moisture-zone distribution. Preliminary analysis showed models using a combination of MAT and MAP performed as well or better than most other possible two-climatic-variable combinations. However, the substitution of MAP with wet and dry season precipitation greatly improved the accuracy of our models, especially in areas where seasonal precipitation patterns are markedly different from annual values (Price and others, 2012).

3.4. Results

3.4.1. Current Moisture-Zone Projections and Model Evaluation

Overall, the current broad geographical pattern of potential moisture-zone distribution across the Hawaiian landscape was well replicated using our three predictors (fig. 3.5). The accuracy of our landscape model based on our calibrated multi-moisture-zone projections for current climate was very high (0.938±0.002 s.d.). An error matrix comparing our mean current projection with the original moisture-zone baseline map shows what types of errors were most common in our projections (table 3.2). Overall, the dry moisture zone was our most accurately predicted moisture zone (0.957 accuracy), and the mesic zone was our least accurately predicted moisture zone

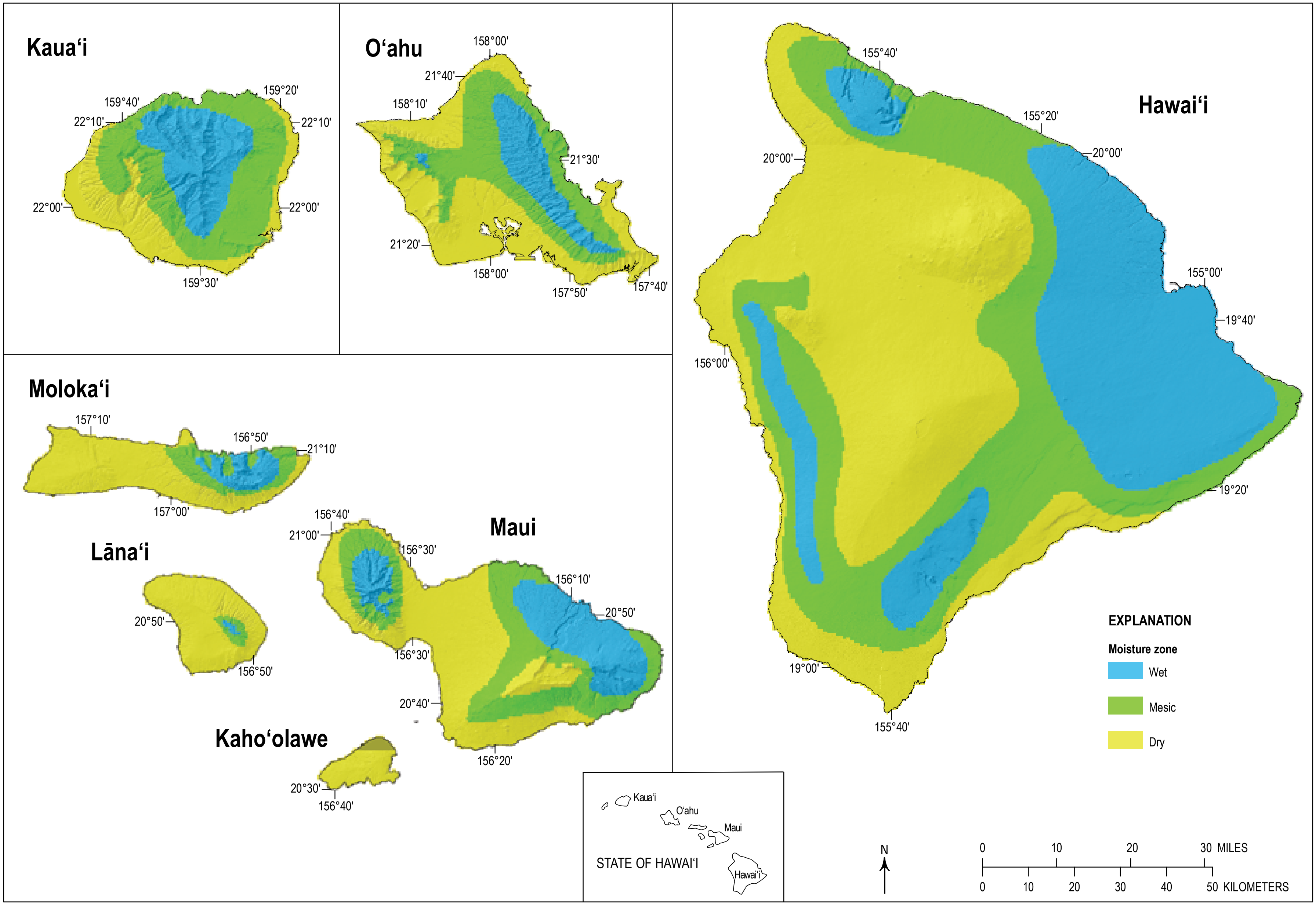

Shaded-relief base modified from U.S. Geological Survey National Elevation Dataset, 2015.

Figure 3.5. Maps showing final landscape moisture-zone projection under current climatic conditions in Hawai‘i.

(0.899 accuracy). Although the general distribution of moisture zones across all islands was well replicated by our model, in a few small areas our model had difficulties in properly representing the extent of certain moisture-zone features. For instance, our model tended to underestimate the extent of moist areas on the top of the Waianae range on the island of Oʻahu and the mesic areas on the top of the island of Lānaʻi (fig. 3.5). As expected, our ensemble committee agreement shows transition zones between moisture zones as areas of greater uncertainty in our current projections, but owing to the high accuracy of our models these areas are generally small (fig. 3.6). Additionally, several areas across the Island of Hawaiʻi also have relatively low within-model agreement, indicating greater uncertainties in our projections. Because of the high overall model accuracy, the uncalibrated current projections showed very small differences in prevalence among moisture zones when compared to the original basemap (table 3.2). Fortunately, our model calibration algorithm was able to reduce these small biases by adding small calibration constants (<5 percent adjustments) without any change in the overall classification accuracy. In preliminary models where biases in projections were larger, the calibration routine effectively removed bias and consequently raised model accuracies.

3.4.2. Future Moisture-Zone Projections Across the Archipelago and Individual Islands

Our future moisture-zone projection shows the suitability of the Hawaiian landscape to moisture zones by the end of the century (fig. 3.7). Our model-agreement map for future projections shows the uncertainty in projections is also concentrated in ecotones (fig. 3.8). Differences between figures 3.3 and 3.5 highlight areas that, by the end of the century, are projected to become more climatically suitable to a moisture zone other than the one present today. In quantitative terms, the extent of mesic areas across the archipelago is projected to decrease by 32 percent, with smaller extent increases for both dry and wet habitats (table 3.3). Although the decrease in the extent of mesic areas is large, this value hides an even greater underlying shift in distribution of mesic forest areas across the state where, by the end of the century, only 45 percent of current mesic areas are projected to remain in mesic conditions. This difference between mesic-extent change and projected areas remaining in mesic conditions is due to some of the loss in current mesic areas being counterbalanced by transition into mesic conditions in some other areas by the end of the century (table 3.4).

Table 3.2. Comparison of actual and modeled baseline moisture-zone prevalence as a proportion of total land area across the seven main Hawaiian Islands.

Moisture zone	Actual baseline prevalence	Predicted baseline prevalence:	
		Uncalibrated model	Calibrated model
Dry	0.451	0.446	0.449
Mesic	0.292	0.300	0.295
Wet	0.256	0.255	0.256

Table 3.3. Summary of projected shifts in moisture-zone extent and prevalence between current and projected future conditions.

Moisture zone	Current area (km^2)	Projected future area (km^2)	Current proportion of land area	Projected future proportion of land area	Percent change in total area	Percent of current area unchanged
Dry	7,290	8,440	0.449	0.52	15.78	88.9
Mesic	4,790	3,270	0.295	0.201	-31.73	45.2
Wet	4,160	4,540	0.256	0.279	8.98	92.0

Table 3.4. Transition matrix illustrating the amount of area shifting among moisture-zone classes between current and projected future conditions.

Future moisture zone	Projected future area (km^2) by source moisture zone			Total projected future area (km^2)
	Dry	Mesic	Wet	
Dry	6,483	1,925	32	8,440
Mesic	800	2,164	303	3,270
Wet	9	700	3,829	4,540

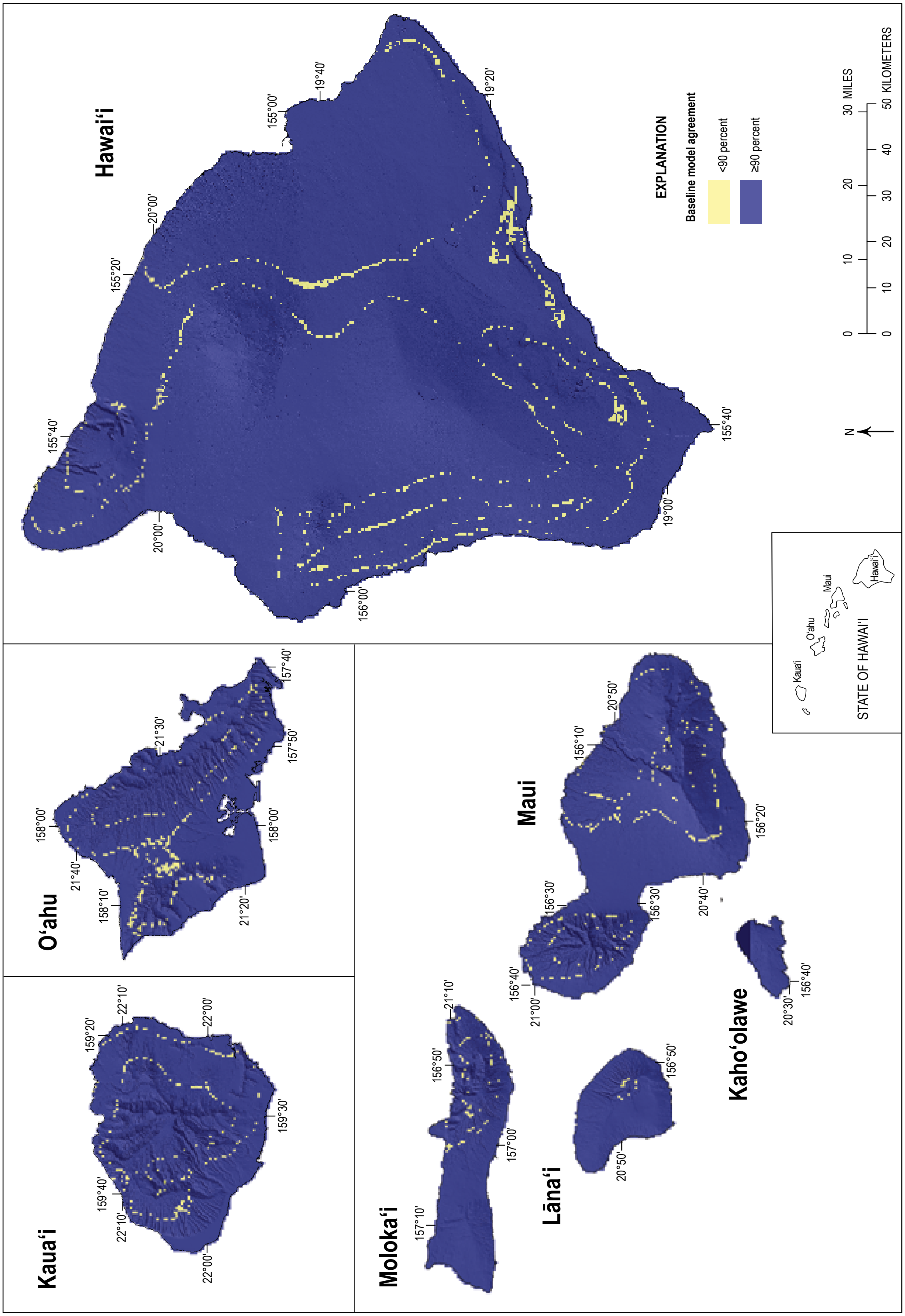

Figure 3.6. Maps showing agreement among 200 iterations of current landscape moisture-zone projections in Hawai‘i.

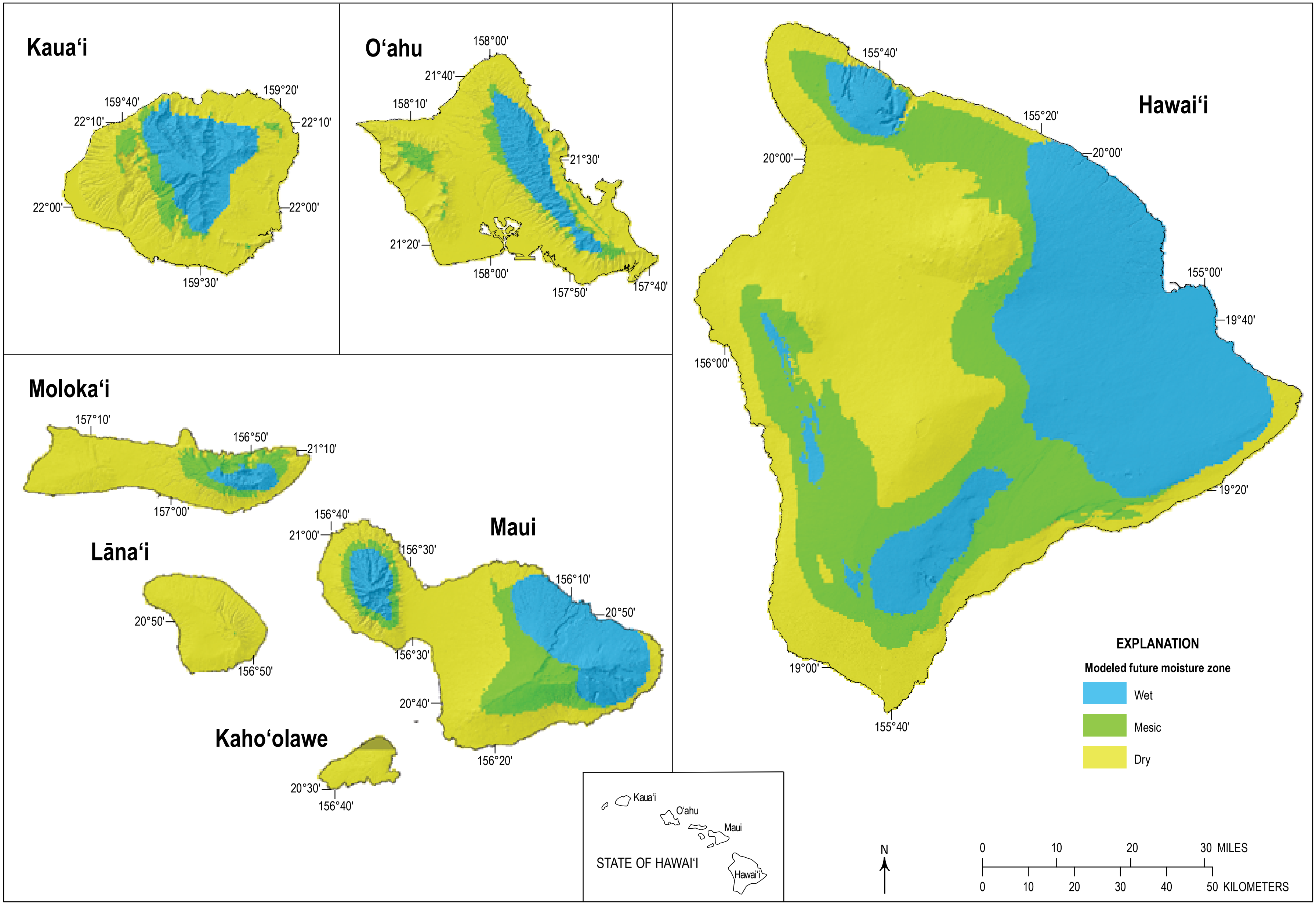

Shaded-relief base modified from U.S. Geological Survey National Elevation Dataset, 2015.

Figure 3.7. Maps showing final landscape moisture-zone projection under future climatic conditions in Hawai‘i.

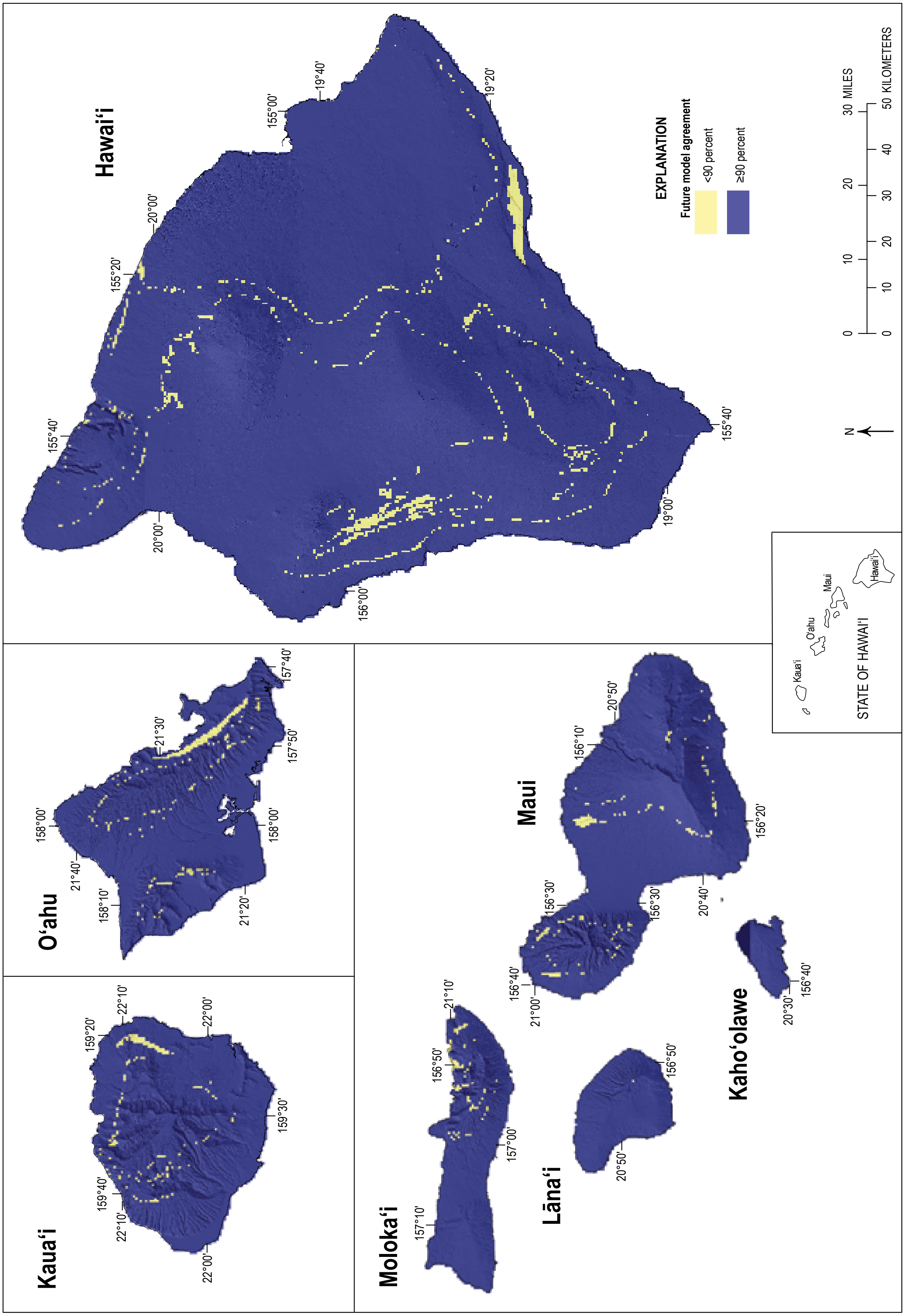

Shaded-relief base modified from U.S. Geological Survey National Elevation Dataset, 2015.

Figure 3.8. Maps showing agreement among 200 iterations of future landscape moisture-zone projections.

3.4.3. Projected Moisture-Zone Shifts Across Islands

The analysis of moisture-zone changes by individual island groups (Kauaʻi, Oʻahu, Maui Nui [the islands of Maui, Molokaʻi, Lānaʻi, and Kahoʻolawe], and Hawaiʻi) shows considerable variability in projected change in the prevalence of the three moisture zones across islands (figs. 3.9, 3.10). In terms of changes in overall extent of moisture zones across islands (fig. 3.9), both Oʻahu and Kauaʻi are projected to see large increases in the extent of dry moisture-zone areas (>50 percent gain), with related large decreases in mesic moisture-zone areas (>75 percent loss). However, this overall change in moisture-zone extent hides drastic changes in the distribution of the mesic moisture zone across the islands. The results summarizing the proportion of current moisture zones left unchanged between now and the end of the century show that nearly 50 percent of current mesic moisture-zone areas on Maui and Hawaiʻi Island by the end of the century become more suitable for dry or wet moisture zones (fig. 3.10). On Kauaʻi and Oʻahu this shift is even more extreme, with less than 25 percent of current mesic moisture-zone areas persisting by the end of the century.

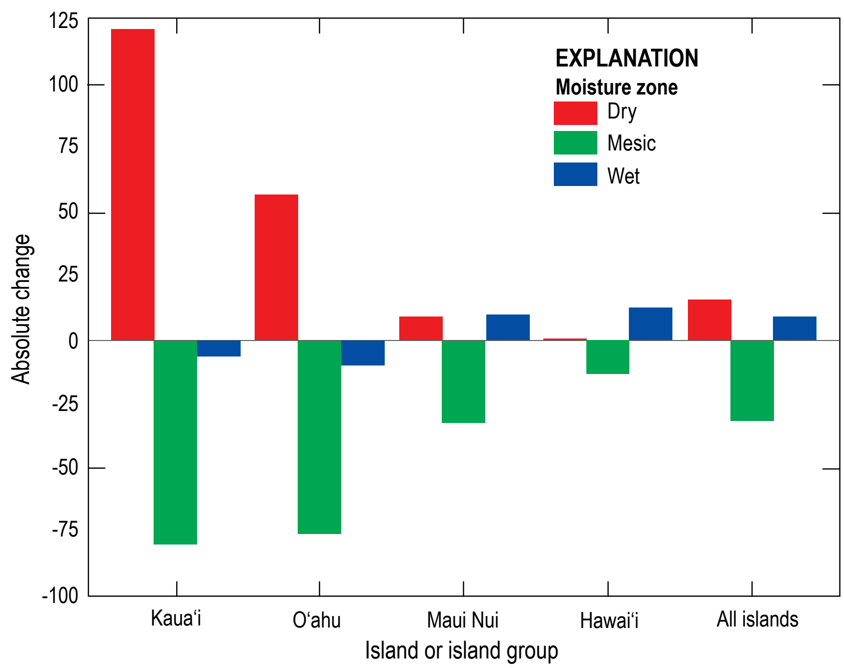

Figure 3.9. Plot of differences in projected proportional change in moisture-zone extent among islands. A value of 0 denotes no change in extent for a moisture zone. Maui Nui includes the islands of Maui, Molokaʻi, Lānaʻi, and Kahoʻolawe.

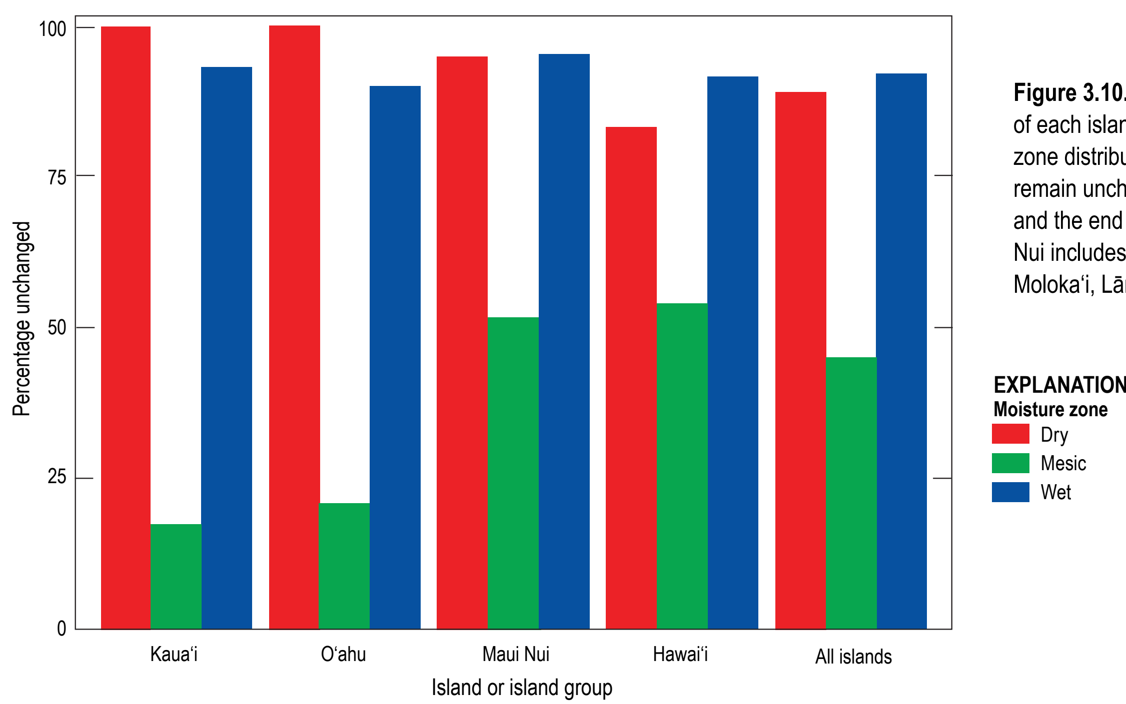

Figure 3.10. Plot of proportion of each island's current moisture-zone distribution projected to remain unchanged between now and the end of the century. Maui Nui includes the islands of Maui, Molokaʻi, Lānaʻi, and Kahoʻolawe.

3.4.4. Translating Moisture-Zone Shifts into Climate-Based Land-Cover Shifts

In the context of broad cover types currently present across the Hawaiian chain, interesting patterns emerge in projected moisture-zone changes (figs. 3.11, 3.12). The loss of mesic areas and increase in dry areas across the archipelago happens primarily in areas currently forested, followed by smaller areas in grasslands. More specifically, the shift towards the dry moisture zone does is not manifested equally across the three vegetation classes (table 3.5). Nearly all mesic-moisture-zone loss within forested areas results from mesic forest switching to dry forest. Similarly, three quarters of the extent loss in mesic moisture zone within grasslands is attributed to a dry grassland expansion. However, the overall contraction of mesic moisture zones within shrubland areas, albeit small, is attributed to shifts towards wet shrubland vegetation. Looking at island differences for these shifts, the slight increase in extent of wet moisture-zone areas across the archipelago mostly happens in shrublands on the Island of Hawaiʻi (fig. 3.13).

3.5. Discussion

Based on the relatively high accuracy of our current model projections, the distribution of moisture zones across the landscape seems strongly related to average climatic conditions. This is partially expected, as moisture zones are clearly dependent on atmospheric climate (Price and others, 2012). The small number of classes and the coarse (500-m) scale of analysis also likely helped with minimizing fine-scale variation that would otherwise not be easily explained by our simple correlative model. With these strong moisture-zone–climate relationships, we were able to recreate and project the Hawaiian moisture zones using climatic variables different from the information used to create the original moisture-zone maps and that are not available for future climate scenarios.

By applying our models to projected end-of-century climate conditions, we are able to provide a first approximation of how the distribution of moisture zones is likely to shift. Except for the large contraction of the wet moisture zone on the west side of Hawaiʻi Island, wet moisture zones are projected to remain relatively unchanged between now and the end of the century in both distribution and extent across the seven main Hawaiian Islands. This is also largely the case for current dry moisture zones except for some dry moisture-zone areas in Hawaiʻi Island displaced by the upward movement of mesic moisture zones. The large contractions of mesic areas across the state follow an increasing pattern from Hawaiʻi to Kauaʻi, with most of these areas shifting towards drier moisture zones.

3.5.1. Understanding Model Errors and Uncertainties

Particularly noteworthy areas of consistent model error include small wet areas on top of Oʻahu and Lānaʻi known to be influenced by fog interception (Ekern, 1964). Indeed, these areas of model discrepancy may be useful to identify locations where factors beyond those directly related to temperature and precipitation may drive differences in plant-available moisture across the archipelago. For instance, relative humidity has been shown to be a strong determinant of tree-line position at higher elevations on Maui (Crausbay and others, 2014). Substrate age and other non-climatic factors may also be important to explain other model discrepancies and patterns at finer spatial scales (Price and others, 2012).

Although our model replicates the pattern of potential moisture-zone distribution across the Hawaiian landscape well, it is still worthwhile to explore the reasons for discrepancies between the model and our original baseline moisture-zone map. First, our approach requires a relevant set of environmental predictors. Although we assessed multiple possible combinations of climatic indicators commonly used in similar analyses, these bioclimatic variables are entirely based on precipitation and temperature and do not account for climate extremes that may be important

Table 3.5. Summary of projected shifts in land-cover class based on integrating moisture-zone shifts with current distribution of forest, shrubland, and grassland areas.

Land-cover class	Current percent of land area	Projected future percent of land area	Percent change from current	Percent unchanged from current
Dry forest	5.1	9.8	94.3	92.5
Mesic forest	11.6	6.3	-45.4	41.0
Wet forest	18.8	19.3	2.7	92.8
Dry shrubland	8.8	9.0	2.4	85.4
Mesic shrubland	5.4	4.3	-20.3	53.5
Wet shrubland	2.4	3.2	37.0	93.0
Dry grassland	9.0	10.6	17.6	93.1
Mesic grassland	6.4	4.4	-31.7	51.9
Wet grassland	1.5	2.0	30.5	71.0

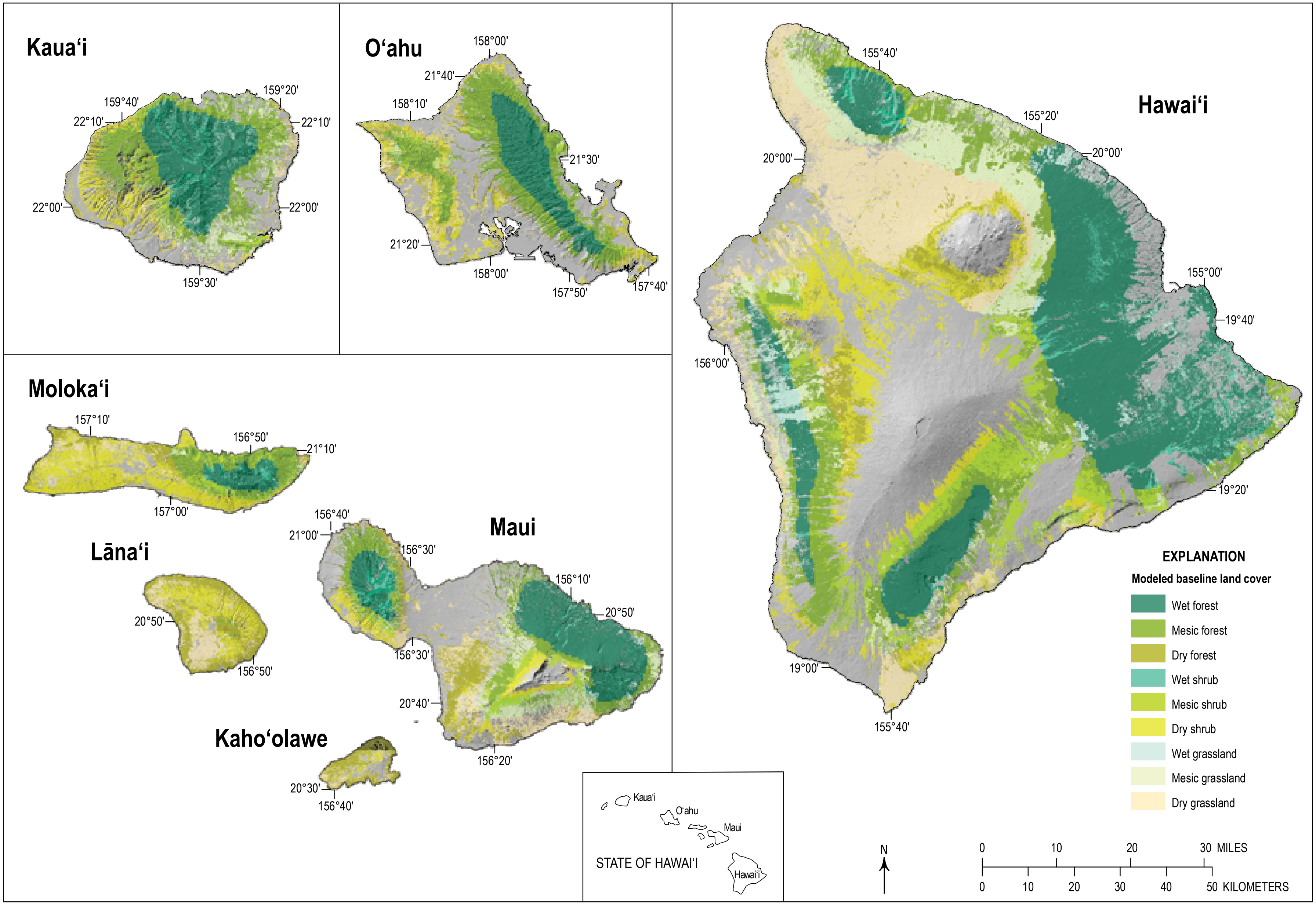

Shaded-relief base modified from U.S. Geological Survey National Elevation Dataset, 2015.

Figure 3.11. Maps showing integration of final landscape moisture-zone projection under current climatic conditions (fig. 3.4) with current forest, shrubland, and grassland classification derived from the carbon assessment for Hawai‘i land-cover map.

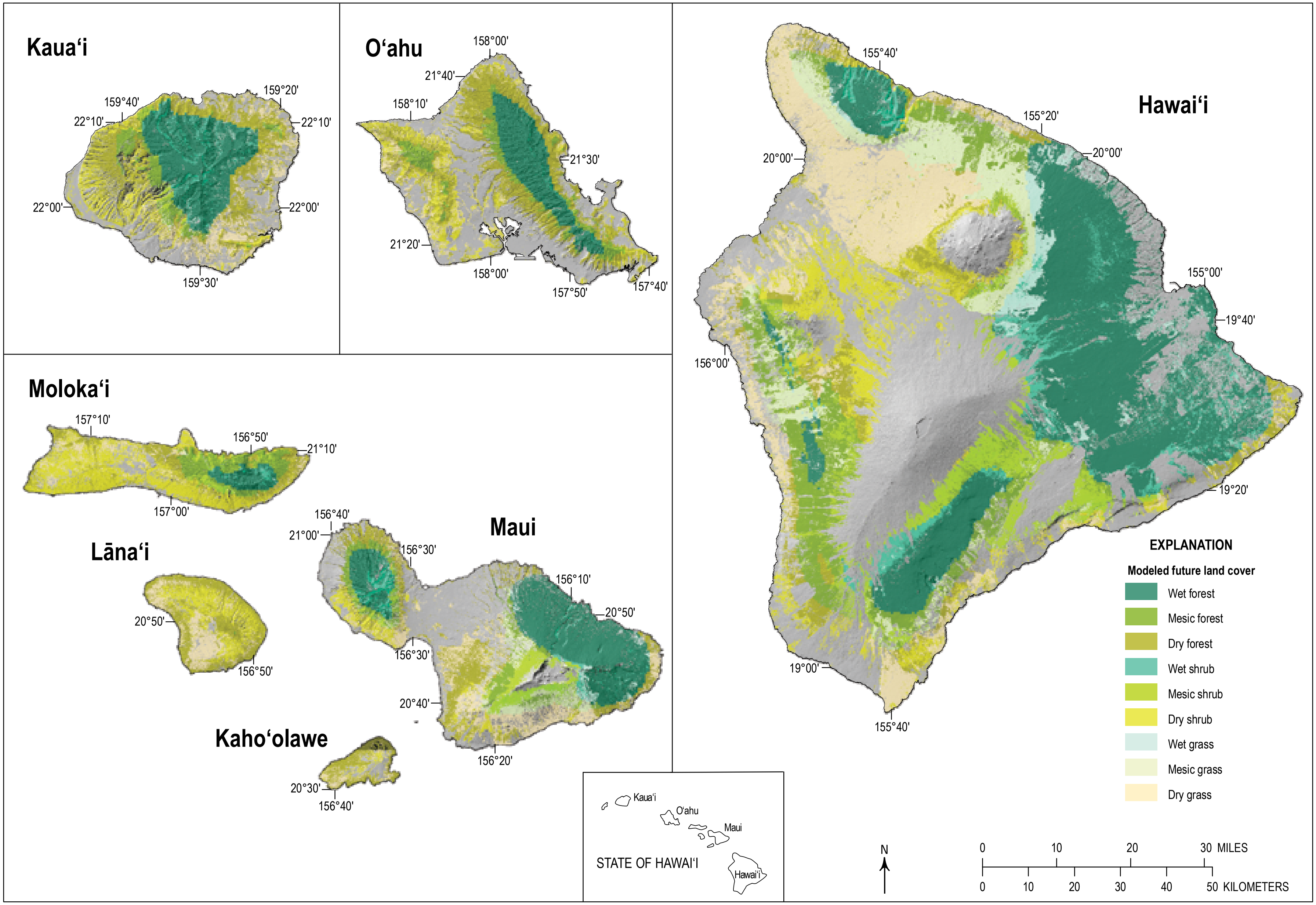

Shaded-relief base modified from U.S. Geological Survey National Elevation Dataset, 2015.

Figure 3.12. Maps showing integration of final landscape moisture-zone projection under future climatic conditions (fig. 3.4) based on current forest, shrubland, and grassland classification derived from the carbon assessment for Hawai‘i land-cover product. Comparison with figure 3.11 gives a preliminary indication of the differential impact of moisture-zone shifts across broad vegetation classes in Hawai‘i.

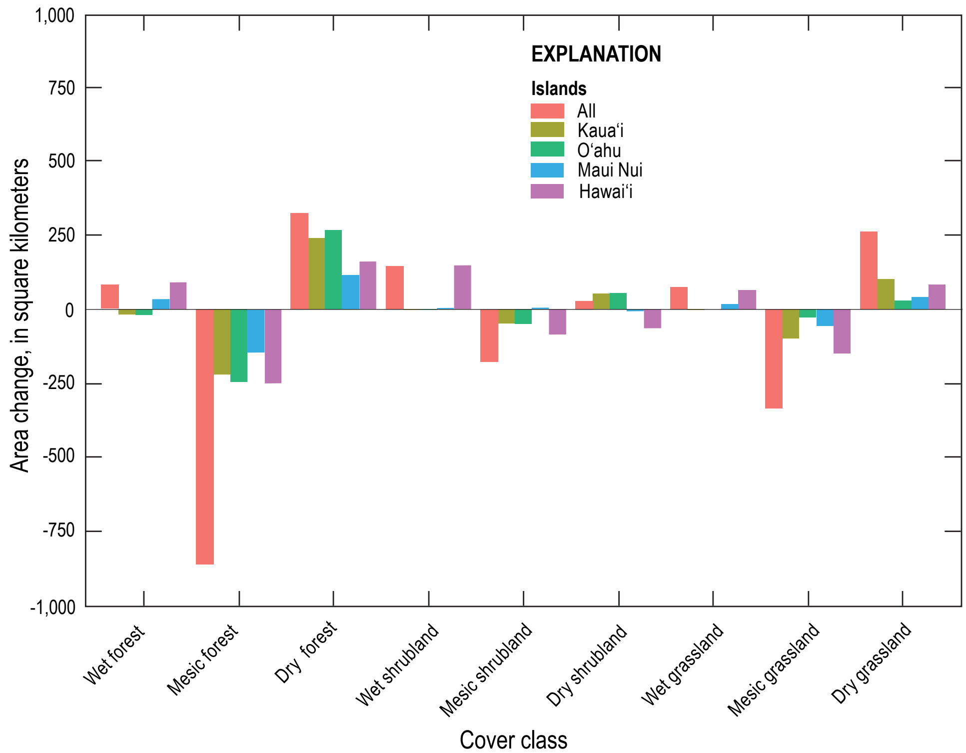

Figure 3.13. Plot of projected area change in moisture-zone extent among broad island vegetation classes. Maui Nui includes the islands of Maui, Molokaʻi, Lānaʻi, and Kahoʻolawe.

in defining landscape vegetation patterns (Crausbay and others, 2014). For example, cloud cover, potential evapotranspiration, and fog deposition are all additional variables that may be important in better defining the distribution of Hawaiian moisture zones; however, these variables are notoriously difficult to estimate for the current climate and even harder to adequately project into the future (Hawkins and Sutton, 2011; Knutti and Sedláček, 2013). Another source of model errors may be inaccuracies in the moisture-zone data used. Indeed, the moisture-zone map is partially based on past archipelago maps of mean annual precipitation (Giambelluca and others, 1986) that are known to have discrepancies when compared to more recent estimates (Giambelluca and others, 2013). Nevertheless, we expect errors in the baseline moisture-zone map to be relatively small given the coarse scale of our analysis.

Regarding future projection uncertainties, our ensemble committee-agreement map (that represents an estimate of model agreement among multiple iterations) only encapsulates a portion of the uncertainty inherent in future projections. Future expansion of this analysis with additional climate projection scenarios, as they are made available, will likely show a much more complete picture of future projection uncertainty. Nevertheless, preliminary analyses using alternative modeling approaches and alternative baselines yielded consistent trends of increases in dry and wet areas at the expense of mesic areas. This indicates that projection uncertainty owing to model choice and starting conditions is not unacceptably large.

3.5.2. Projected Moisture-Zone Shifts in the Context of Hawaiian Climate Trends

In general, the projected moisture-zone shifts follow broad patterns of current and projected climate trends. Projected precipitation shifts are generally expected to make wet areas wetter and dry areas drier, both at the global and regional level (Zhang and others, 2012; Collins and others, 2013). However, examining the differences among islands shows that patterns in our moisture-zone projections are slightly more complex. Namely, expansion of the wet moisture zone occurs on windward (wet) Hawaiʻi and Maui but not on Oʻahu or Kauaʻi. Conversely, expansion of the dry moisture zone occurs on the leeward (dry) side of every island except Hawaiʻi. This larger expansion of the dry moisture zones at the northwestern end of the archipelago matches coarse global future projections of precipitation change (Keener and others, 2012). These projected drying trends also occur in the context of recent decreases in streamflow (Bassiouni and Oki, 2013) and precipitation (Chu and Chen, 2005; Krushelnycky and others, 2013).

One major uncertainty in our moisture-zone-shift projections is the high-elevation areas on Maui and Hawaiʻi influenced by the trade-wind inversion. The frequency and intensity of the trade-wind inversion is known to raise temperatures and cap cloud formation in areas above 2,000 m in elevation, and hence raise insolation and decrease precipitation and relative humidity (Cao and others, 2007). This feature of Hawaiian climate has a major impact on the distribution of vegetation at higher elevations, effectively limiting the height of the forest line on these islands (Kitayama and Mueller-Dombois, 1992; Loope and Giambelluca, 1998). Until recently, there has been considerable debate about the response of trade-wind inversions to regional and global climate shifts (Still and others, 1999; Sperling and others, 2004), but global and regional analysis increasingly point to a likely increase in frequency of the trade-wind inversion that would lead to persistently drier conditions (Lauer and others, 2013; Crausbay and others, 2014).

Although the HRCM simulations replicate the patterns of increased temperature and decreased precipitation in areas above the trade-wind inversion (Zhang and others, 2012), contrary to expected changes in the trade-wind inversion from other analyses, HRCM future projections seem to include a more varied pattern of precipitation change for areas above the trade-wind inversion including areas with more, less, or equal precipitation. This makes some of the projected spread of the wet moisture zone in high-elevation windward Maui and Hawai‘i and the conversion of the top of Maui from dry to mesic likely optimistic.

3.5.3. Temperature-Induced Drought and Vegetation Change

The general increase in dry areas and decrease in mesic areas between present and the end of the century occur in areas that suggest some of these trends will be driven by expected temperature increases. In fact, there is ample research that documents temperature amplification of plant stress and drought (Kolb and Robberecht, 1996; Barber and others, 2000; Park Williams and others, 2013) through greater evapotranspirative demand (Weiss and others, 2009). Recent research has shown that temperature is a strong driver of drought conditions across the southwestern United States including in temperate forests (Barber and others, 2000; Park Williams and others, 2013). Many other studies further highlight the importance of temperature to drought impacts in terms of mortality, stress, and overall vegetation change (Adams and others, 2009; Weiss and others, 2009; Allen and others, 2010; McDowell and others, 2011).

3.5.4. Implications of Projected Vegetation Change to Hawaiian Conservation Efforts

The generally large projected decreases in mesic areas across the state and especially on the islands of Kaua‘i and O‘ahu, have potentially large implications relative to conservation of highly valuable native-species habitat. Mesic habitats in Hawai‘i are zones of high species diversity because they contain elements from both wet and dry habitats (Gagne and Cuddihy, 1990; Price, 2004; Gon, 2006). However, because this moisture zone is optimal for timber production, agriculture, and ranching, large parts of this habitat have been altered from their natural condition, resulting in a loss of native-species diversity.

The reduction in extent of the mesic zone is directly linked to an increase in the future extent of dry habitat. Although the original Hawaiian dry-plant communities were also known to harbor a great diversity of plant species, particularly woody taxa (Rock, 1913; Gagne and Cuddihy, 1990), much of this habitat zone, particularly below 1,000-m elevation, has already been substantially altered by human land use, invasive species, and fire. An expansion of the area of dry habitat will likely result in an increase in areas impacted by fire, which are then quickly colonized by invasive grass species, and the likelihood of more fires further increases. When a fire starts in a dry habitat, it can easily spread into the adjacent mesic habitats and cause substantial damage to the species composition and vegetation structure of that community. Beyond the broad categorical projected shift of mesic areas to dry areas, most of the existing native dry communities are on the wetter end of the dry moisture zone range, which suggests impacts of projected climate shifts within stable moisture-zone areas may also be significant.

Besides the significant pattern of mesic-to-dry moisture-zone switch projected in our models, one other projected change with clear conservation implication is the likelihood of the nearly complete loss of the wet forest habitat on the western side of the Island of Hawai‘i. Although the reduction of the wet forest in this area is spatially compensated by projected wet zone expansion at higher elevation windward areas on Hawai‘i Island, the native plant species adapted to the wet habitat in the Kona area (for example, *Cyanea marksii* and *Cyrtandra menziesii*) will likely be lost (Price, 2004).

Our newly designed approach opens the door to several improvements to vegetation and habitat modeling in Hawai‘i and elsewhere. We are currently refining our modeling approach to consider differences in limiting factors to the distribution of individual vegetation classes. We are also exploring modeling improvements that would allow for the consideration of finer vegetation classes that are more easily relatable to on-the-ground management efforts. With these and other improvements, we can use our models as a steppingstone to develop mechanistic models for the region that can provide a wealth of information on the processes that drive the projected shifts our analysis identifies.

Nevertheless, our projections can still be used to characterize coarse vegetation changes and the long-term consequences to carbon storage across the landscape. To do so, the integration of our projections with multiple fire, landscape-management, and use scenarios, along with the assessment of aboveground and belowground carbon storage will provide an unprecedented detail of carbon stocks across the Hawaiian landscape and the potential future shifts. As such, our results are used in Sleeter and others (this volume, chap. 8) to refine land-use and land-cover scenarios for the archipelago and project terrestrial carbon storage and CO_2 fluxes.

3.6. References Cited

Adams, H.D., Guardiola-Claramonte, M., Barron-Gafford, G.A., Villegas, J.C., Breshears, D.D., Zou, C.B., Troch, P.A., and Huxman, T.E., 2009, Temperature sensitivity of drought-induced tree mortality portends increased regional die-off under global-change-type drought: Proceedings of the National Academy of Sciences, v. 106, no. 17, p. 7063–7066.

Allen, C.D., Macalady, A.K., Chenchouni, H., Bachelet, D., McDowell, N., Vennetier, M., Kitzberger, T., Rigling, A., Breshears, D.D., Hogg, E.H., Gonzalez, P., Fensham, R., Zhang, Z., Castro, J., Demidova, N., Lim, J.-H., Allard, G., Running, S.W., Semerci, A., and Cobb, N., 2010, A global overview of drought and heat-induced tree mortality reveals emerging climate change risks for forests: Forest Ecology and Management, v. 259, no. 4, p. 660–684, available at http://dx.doi.org/10.1016/j.foreco.2009.09.001.

Asner, G.P., Elmore, A.J., Hughes, R.F., Warner, A.S., Vitousek, P.M., 2005, Ecosystem structure along bioclimatic gradients in Hawai‘i from imaging spectroscopy: Remote Sensing of Environment, v. 96, p. 497–508.

Asner, G.P., Hughes, R.F., Varga, T.A., Knapp, D.E., and Kennedy-Bowdoin, T., 2009, Environmental and biotic controls over aboveground biomass throughout a tropical rain forest: Ecosystems, v. 12, no. 2, p. 261–278, available at http://dx.doi.org/10.1007/s10021-008-9221-5.

Asner, G.P., Hughes, R.F., Mascaro, J., Uowolo, A.L., Knapp, D.E., Jacobson, James, Kennedy-Bowdoin, T., and Clark, J.K., 2011, High-resolution carbon mapping on the million-hectare Island of Hawaii: Frontiers in Ecology and the Environment, v. 9, no. 8, p. 434–439, available at http://dx.doi.org/10.1890/100179.

Asner, G.P., Hughes, R.F., Vitousek, P.M., Knapp, D.E., Kennedy-Bowdoin, T., Boardman, J., Martin, R.E., Eastwood, M., and Green, R.O., 2008, Invasive plants transform the three-dimensional structure of rain forests: Proceedings of the National Academy of Sciences, v. 105, no. 11, p. 4519–4523.

Bachelet, D., Neilson, R.P., Lenihan, J.M., and Drapek, R.J., 2001, Climate change effects on vegetation distribution and carbon budget in the United States: Ecosystems, v. 4, no. 3, p. 164–185.

Barber, V.A., Juday, G.P., and Finney, B.P., 2000, Reduced growth of Alaskan white spruce in the twentieth century from temperature-induced drought stress: Nature, v. 405, p. 668–673.

Bassiouni, M., and Oki, D.S., 2013, Trends and shifts in streamflow in Hawai‘i, 1913–2008: Hydrologic Processes, v. 27, no. 10, p. 1484–1500, available at http://dx.doi.org/10.1002/hyp.9298.

Beniston, M., Diaz, H.F., and Bradley, R.S., 1997, Climatic change at high elevation sites—an overview: Climate Change, v. 36, no. 3, p. 233–251.

Benoit, J.W., Fujioka, F.M., and Weise, D.R., 2009, Modeling fire behavior on tropical islands with high-resolution weather data, in González-Cabán, A., ed., Proceedings of the Third International Symposium on Fire Economics, Planning, and Policy—Common Problems and Approaches: Albany, Calif., U.S. Department of Agriculture, Forest Service, Pacific Southwest Research Station General Technical Report PSW-GTR-227, p. 321–330.

Bonan, G.B., Levis, S., Sitch, S., Vertenstein, M., and Oleson, K.W., 2003, A dynamic global vegetation model for use with climate models—concepts and description of simulated vegetation dynamics: Global Change Biology, v. 9, no. 11, p. 1543–1566.

Cao, G., Giambelluca, T.W., Stevens, D.E., and Schroeder, T.A., 2007, Inversion variability in the Hawaiian trade wind regime: Journal of Climate, v. 20, no. 7, p. 1145–1160.

Chu, P.-S., and Chen, H., 2005, Interannual and interdecadal rainfall variations in the Hawaiian islands: Journal of Climate, v. 18, no. 22, p. 4796–4813.

Collins, M., Knutti, R., Arblaster, J., Dufresne, J.-L., Fichefet, T., Friedlingstein, P., Gao, X., Gutowski, W.J., Jr., Johns, T., Krinner, G., Shongwe, M., Tebaldi, C., Weaver, A.J., and Wehner, M., 2013, Long-term climate change—Projections, commitments and irreversibility, *in* Stocker, T.F., Qin, D., Plattner, G.-K., Tignor, M.M.B., Allen, S.K., Boschung, J., Nauels, A., Xia, Y., Bex, V., Midgley, P.M., eds., Climate change 2013 The physical science basis—Contribution of Working Group I to the Fifth Assessment Report of the Intergovernmental Panel on Climate Change: Cambridge, U.K., Cambridge University Press, 108 p.

Cramer, W., Bondeau, A., Woodward, F.I., Prentice, I.C., Betts, R.A., Brovkin, V., Cox, P.M., Fisher, V., Foley, J.A., Friend, A.D., Kucharik, C., Lomas, M.R., Ramankutty, N., Sitch, S., Smith, B., White, A., and Young-Molling, C., 2001, Global response of terrestrial ecosystem structure and function to CO_2 and climate change—results from six dynamic global vegetation models: Global Change Biology, v. 7, no. 4, p. 357–373.

Crausbay, S.D., Frazier, A.G., Giambelluca, T.W., Longman, R.J., and Hotchkiss, S.C., 2014, Moisture status during a strong El Niño explains a tropical montane cloud forest's upper limit: Oecologia, v. 175, no. 1, p. 273–284, available at https://dx.doi.org/10.1007/s00442-014-2888-8.

Diaz, H.F., and Bradley, R.S., 1997, Temperature variations during the last century at high elevation sites: Climatic Change, v. 36, no. 3, p. 253–279.

Ekern, P.C., 1964, Direct interception of cloud water on Lanaihale, Hawaii: Journal of the Soil Science Society of America, v. 28, no. 3, p. 419–421.

Elith, J., Leathwick, J.R., and Hastie, T., 2008, A working guide to boosted regression trees: Journal of Animal Ecology, v. 77, no. 4, p. 802–813.

Ellsworth, L.M., Litton, C.M., Taylor, A.D., and Kauffman, J.B., 2013, Spatial and temporal variability of guinea grass (*Megathyrsus maximus*) fuel loads and moisture on Oahu, Hawaii: International Journal of Wildland Fire, v. 22, no. 8, p. 1083–1092, available at http://dx.doi.org/10.1071/WF12051.

Fortini, L., Price, J., Jacobi, J., Vorsino, A., Burgett, J., Brinck, K., Amidon, F., Miller, S., Gon, S., III, Koob, G., and Paxton, E., 2013, A landscape-based assessment of climate change vulnerability for all native Hawaiian plants: University of Hawai‘i at Hilo, Hawai‘i Cooperative Studies Unit Technical Report HCSU–044, 134 p., available at http://hdl.handle.net/10790/2620.

Fortini, L.B., Vorsino, A.E., Amidon, F.A., Paxton, E.H., and Jacobi, J.D., 2015, Large-scale range collapse of Hawaiian forest birds under climate change and the need for 21st century conservation options: PLoS ONE, v. 10, no. 10, 22 p., available at http://dx.doi.org/10.1371/journal.pone.0140389.

Gagne, W.C., and Cuddihy, L.W., 1990, Vegetation, *in* Wagner, W.L., Herbst, D.R., and Sohmer, S.H., 1999, Manual of the Flowering Plants of Hawai‘i (2d ed.): Honolulu, University of Hawai‘i Press, Bishop Museum Press, p. 45–114.

Giambelluca, T.W., Chen, Q., Frazier, A.G., Price, J.P., Chen, Y.-L., Chu, P.-S., Eischeid, J.K., and Delparte, D.M., 2013, Online Rainfall Atlas of Hawai‘i: Bulletin of the American Meteorological Society, v. 94, p. 313–316. (Available at http://rainfall.geography.hawaii.edu.)

Giambelluca, T.W., Nullet, M.A., and Schroeder, T.A., 1986, Rainfall atlas of Hawai‘i: Honolulu, Hawai‘i Department of Land and Natural Resources, Division of Water and Land Development Report R76, 267 p.

Giambelluca, T.W., Shuai, X., Barnes, M.L., Alliss, R.J., Longman, R.J., Miura, T., Chen, Q., Frazier, A.G., Mudd, R.G., Cuo, L., and Businger, A.D., 2014, Evapotranspiration of Hawai‘i: final report to the U.S. Army Corps of Engineers—Honolulu District and the Commission on Water Resource Management, State of Hawai‘i, 178 p., available at http://evapotranspiration.geography.hawaii.edu.

Gibbs, H., 2007, Monitoring and estimating tropical forest carbon stocks—making REDD a reality: Environmental Research Letters, v. 2, no. 4, 13 p.

Gon, S.M., III, Allison, A., Cannarella, R.J., Jacobi, J.D., Kaneshiro, K.Y., Kido, M.H., Lane-Kamahele, M., and Miller, S.E., 2006, A GAP analysis of Hawaii—Final Report: U.S. Geological Survey, Research Corporation of the University of Hawai‘i, 163 p., plus maps and appendixes.

Gonzalez, P., Neilson, R.P., Lenihan, J.M., and Drapek, R.J., 2010, Global patterns in the vulnerability of ecosystems to vegetation shifts due to climate change: Global Ecology Biogeography, v. 19, no. 6, p. 755–768, available at http://dx.doi.org/10.1111/j.1466-8238.2010.00558.x.

Hartig, F., Dyke, J., Hickler, T., Higgins, S.I., O’Hara, R.B., Scheiter, S., and Huth, A., 2012, Connecting dynamic vegetation models to data—an inverse perspective: Journal of Biogeography, v. 39, no. 12, p. 2240–2252, available at http://dx.doi.org/10.1111/j.1365-2699.2012.02745.x.

Hastie, T., Tibshirani, R., and Friedman, J., 2011, The Elements of Statistical Learning—Data Mining, Inference, and Prediction (2d ed.): New York, Springer.

Hawkins, E., and Sutton, R., 2011, The potential to narrow uncertainty in projections of regional precipitation change: Climate Dynamics, v. 37, no. 1, p. 407–418, available at http://dx.doi.org/10.1007/s00382-010-0810-6.

Hijmans, R., Phillips, S., Leathwick, J., and Elith, J., 2012, Dismo—Species distribution modeling: Comprehensive R Archive Network, https://cran.r-project.org.

Hijmans, R.J., van Etten, J., Mattiuzzi, M., Sumner, M., Greenberg, J.A., Lamigueiro, O.P., Bevan, A., Racine, E.B., and Shortridge, A., 2014, Raster—Geographic data analysis and modeling: Comprehensive R Archive Network, https://cran.r-project.org.

Jacobi, J.D., 1989, Vegetation maps of the upland plant communities on the islands of Hawai‘i, Maui, Moloka‘i, and Lana‘i: University of Hawai‘i at Mānoa, Cooperative National Park Resources Studies Unit Technical Report 68, 25 p.

Jiménez-Valverde, A., and Lobo, J.M., 2007, Threshold criteria for conversion of probability of species presence to either–or presence–absence: Acta Oecologica, v. 31, no. 3, p. 361–369.

Keener, V.W., Marra, J.J., Finucane, M.L., Spooner, D., and Smith, M.H., eds., 2012, Climate change and Pacific Islands; indicators and impacts—Report for the 2012 Pacific Islands regional climate assessment (PIRCA): Washington, D.C., Island Press, 170 p.

Kitayama, K., and Mueller-Dombois, D., 1992, Vegetation of the wet windward slope of Haleakala, Maui, Hawaii: Pacific Science, v. 46, no. 2, p. 197–220. [Accessed March 3, 2015 at http://scholarspace.manoa.hawaii.edu/handle/10125/722.]

Knutti, R., and Sedláček, J., 2013, Robustness and uncertainties in the new CMIP5 climate model projections: Nature Climate Change, v. 3, no. 4, p. 369–373, available at http://dx.doi.org/10.1038/nclimate1716.

Kolb, P.F., and Robberecht, R., 1996, High temperature and drought stress effects on survival of Pinus ponderosa seedlings: Tree Physiology, v. 16, no. 8, p. 665–672.

Krushelnycky, P.D., Loope, L.L., Giambelluca, T.W., Starr, F., Starr, K., Drake, D.R., Taylor, A.D., and Robichaux, R.H., 2013, Climate-associated population declines reverse recovery and threaten future of an iconic high-elevation plant: Global Change Biology, v. 19, no. 3, p. 911–922, available at http://dx.doi.org/10.1111/gcb.12111.

Lauer, A., Zhang, C., Elison-Timm, O., Wang, Y., and Hamilton, K., 2013, Downscaling of climate change in the Hawai‘i region using CMIP5 results—On the choice of the forcing fields: Journal of Climate, v. 26, no. 24, p. 6–10030, available at http://dx.doi.org/10.1175/JCLI-D-13-00126.1.

Liu, C., White, M., and Newell, G., 2011, Measuring and comparing the accuracy of species distribution models with presence–absence data: Ecography, v. 34, no. 2, p. 232–243, available at http://dx.doi.org/10.1111/j.1600-0587.2010.06354.x.

Loope, L., and Giambelluca, T., 1998, Vulnerability of island tropical montane cloud forests to climate change, with special reference to East Maui, Hawaii: Climatic Change, v. 39, no. 2, p. 503–517.

Lucht, W., Schaphoff, S., Erbrecht, T., Heyder, U., and Cramer, W., 2006, Terrestrial vegetation redistribution and carbon balance under climate change: Carbon Balance and Management, v. 1, no. 6, 7 p.

Mascaro, J., Becklund, K.K., Hughes, R.F., and Schnitzer, S.A., 2008, Limited native plant regeneration in novel, exotic-dominated forests on Hawai‘i: Forest Ecology and Management, 256, no. 4, p. 593–606.

McDowell, N.G., Beerling, D.J., Breshears, D.D., Fisher, R.A., Raffa, K.F., and Stitt, M., 2011, The interdependence of mechanisms underlying climate-driven vegetation mortality: Trends in Ecology and Evolution, v. 26, no. 10, p. 523–532, available at http://dx.doi.org/10.1016/j.tree.2011.06.003.

Ostertag, R., Inman-Narahari, F., Cordell, S., Giardina, C.P., and Sack, L., 2014, Forest structure in low-diversity tropical forests—A study of Hawaiian wet and dry forests: PLoS ONE, v. 9, no. 8, 18 p., available at http://dx.doi.org/10.1371/journal.pone.0103268.

Park Williams, A., Allen, C.D., Macalady, A.K., Griffin, D., Woodhouse, C.A., Meko, D.M., Swetnam, T.W., Rauscher, S.A., Seager, R., Grissino-Mayer, H.D., Dean, J.S., Cook, E.R., Gangodagamage, C., Cai, M., and McDowell, N.G., 2013, Temperature as a potent driver of regional forest drought stress and tree mortality: Nature Climate Change, v. 3, p. 292–297, available at http://dx.doi.org/10.1038/nclimate1693.

Pavlick, R., Drewry, D.T., Bohn, K., Reu, B., and Kleidon, A., 2013, The Jena Diversity-Dynamic Global Vegetation Model (JeDi-DGVM)—A diverse approach to representing terrestrial biogeography and biogeochemistry based on plant functional trade-offs: Biogeosciences, v. 10, no. 6, p. 4137–4177, available at http://dx.doi.org/10.5194/bg-10-4137-2013.

Price, J.P., 2004, Floristic biogeography of the Hawaiian Islands—influences of area, environment and paleogeography: Journal of Biogeography, v. 31, no. 3, p. 487–500.

Price, J.P., Gon, S.M., III, Jacobi, J.D., and Matsuwaki, D., 2007, Mapping plant species in ranges in the Hawaiian Islands—Developing a methodology and associated GIS layers: University of Hawai‘i at Hilo, Hawai‘i Cooperative Studies Unit Technical Report HCSU–008, 58 p., available at http://hdl.handle.net/10790/2687.

Price, J.P., Jacobi, J.D., Gon, S.M., III, Matsuwaki, D., Mehrhoff, L., Wagner, W., Lucas, M., and Rowe, B., 2012, Mapping plant species ranges in the Hawaiian Islands—Developing a methodology and associated GIS layers: U.S. Geological Survey Open-File Report 2012–1192, 34 p., 1 appendix (species table), 1,158 maps, available at http://pubs.usgs.gov/of/2012/1192/.

Rangwala, I., Sinsky, E., and Miller, J.R., 2013, Amplified warming projections for high altitude regions of the northern hemisphere mid-latitudes from CMIP5 models: Environmental Research Letters, v. 8, no. 2, 9 p., available at http://dx.doi.org/10.1088/1748-9326/8/2/024040

R Core Team, 2014, R—A language and environment for statistical computing: Vienna, Austria, R Foundation for Statistical Computing, https://www.r-project.org.

Ridgeway, G., 2005, Generalized boosted models—A guide to the gbm package.

Rock, J.F., 1913, The indigenous trees of the Hawaiian Islands: Honolulu, privately published.

Rollins, M.G., 2009, LANDFIRE: A nationally consistent vegetation, wildland fire, and fuel assessment: International Journal of Wildland Fire, v. 18, p. 235–249.

Sperling, F.N., Washington, R., and Whittaker, R.J., 2004, Future climate change of the subtropical North Atlantic—implications for the cloud forests of Tenerife: Climatic Change, v. 65, no. 1, p. 103–123.

Still, C.J., Foster, P.N., and Schneider, S.H., 1999, Simulating the effects of climate change on tropical montane cloud forests. Nature, v. 398, p. 608–610.

Tovar, C., C.A. Arnillas, Cuesta, F., and Buytaert, W., 2013, Diverging responses of tropical Andean biomes under future climate conditions: PLoS ONE, v. 8, no. 5, 12 p., available at http://dx.doi.org/10.1371/journal.pone.0063634.

Weiss, J.L., Castro, C.L., and Overpeck, J.T., 2009, Distinguishing pronounced droughts in the Southwestern United States—seasonality and effects of warmer temperatures: Journal of Climate, v. 22, no. 22, p. 5918–5932 available at http://dx.doi.org/10.1175/2009JCLI2905.1.

Zhang, C., Wang, Y., Lauer, A., and Hamilton, K., 2012, Configuration and evaluation of the WRF model for the study of Hawaiian regional climate: Monthly Weather Review, v. 140, no. 10, p. 3259–3277, available at http://dx.doi.org/10.1175/MWR-D-11-00260.1.

Ziegler, A.C., 2002, Hawaiian Natural History, Ecology, and Evolution: Honolulu, University of Hawaii Press, 477 p.